Layered mafic sill complex beneath the eastern Snake River Plain: Evidence from cyclic geochemical variations in basalt

John W. Shervais Department of Geology, Utah State University, Logan, Utah 84322-4505, USA
Scott K. Vetter Department of Geology, Centenary College, Shreveport, Louisiana 71104-1188, USA
Barry B. Hanan Department of Geological Sciences, San Diego State University, San Diego, California 92182-1020, USA

ABSTRACT

The eastern Snake River Plain in southern Idaho, western United States, is characterized by 1–2 km of Pleistocene to late Pliocene basalt overlying rhyolite caldera complexes. Cyclic variations in the chemical composition of basalts from 1136 m of scientific drill core show that the parent magmas of these lavas evolved by crystal fractionation at shallow to intermediate crustal depths, punctuated by episodic recharge with more primitive compositions and assimilation of adjacent wall rock. We have identified 10 upward fractionation cycles and four reversed cycles; assimilation of sialic crust was limited and mainly affects the oldest basalts, which directly overlie rhyolites. We infer that the crystal fractionation and/or recharge cycles took place in a series of sill-like intrusions at intermediate crustal depths that now form a layered mafic intrusion that underlies the eastern Snake River Plain at depth. This layered sill complex is represented by the ~10-km-thick "basaltic sill" that has been imaged seismically at ~12–22 km depth. The association of this mid-crustal sill complex with geochemical fractionation cycles in basalt supports the concept that exposed layered mafic intrusions may be linked to overlying basalt provinces that have since been removed by erosion.

Keywords: basaltic volcanism, basalt, layered intrusions, crustal structure.

INTRODUCTION

Petrologists have long used layered mafic intrusions to infer magmatic liquid lines of descent and to speculate about processes that control the compositions of volcanic rocks erupted at the surface. The most important processes inferred from layered mafic intrusions include crystal fractionation (by gravitational settling or crystallization fronts at the base and sides of the magma chamber), magma recharge and mixing, and the progressive assimilation of roof or wall rocks (e.g., Wager and Brown, 1967; Irvine, 1970; Jackson, 1970, 1971; McBirney and Noyes, 1979; Pallister and Hopson, 1981). Petrologists invoke these processes to explain chemical variations observed in lavas erupted on the Earth's surface, but it is rarely possible to relate these processes to stratigraphic successions of lava in a way that correlates with the multiple cycles of fractionation, recharge, and mixing observed in layered mafic intrusions.

We document here a 1136-m-thick stratigraphic section of basalt sampled by scientific drilling that preserves geochemical variations consistent with crystal fractionation, magma recharge, and assimilation in a layered magma chamber at mid-crustal depths. Upward fractionation sequences are inferred to represent fractional crystallization cycles identified in layered intrusions; reversed intervals are inferred to document progressive recharge of a previously fractionated magma system. The chemical stratigraphy of these basalts provides a clear link between processes inferred from layered mafic intrusions and the chemical evolution of basaltic magmas.

GEOLOGIC RELATIONS

The Yellowstone–Snake River Plain volcanic system of the western United States represents one of the best examples of hotspot volcanism preserved within continental lithosphere, although the significance and origin of the volcanic rocks are controversial (Fig. 1). Rhyolite caldera complexes and their associated ignimbrites are overlain by a thin veneer of basalt, ~1–2 km thick, erupted from small shield volcanoes and cinder cones. Major and trace element systematics of the basalts are consistent with a sublithospheric mantle plume origin, similar to the source of ocean island basalts, but their isotopic compositions reflect an enriched subcontinental mantle lithosphere source (Leeman, 1982; Geist et al., 2002; Hughes et al., 2002; Shervais et al., 2003, 2005). Core from adjacent scientific drill holes NPRE (0–185 m) and WO-2 (cored from 152 to 1515 m total depth) at the Idaho National Laboratory (INL) preserves a nearly complete record of volcanism at this site, comprising 1136 m of basalt overlying 380 m of rhyolite tuff and breccia. Basalts at the surface are dated as ca. 230 ka (Champion et al., 2002). A sediment horizon at 215–233 m depth has been correlated with the Bruhnes-Matuyama magneto-stratigraphic boundary (780 ka), while the magnetic polarity chronozone C2n (Olduvai, ca. 1.81 Ma) occurs at ~526 m depth (Champion et al., 2002; Morse and McCurry, 2002). The underlying rhyolites are correlated with the Heise volcanic complex, the youngest rocks of which have been dated as ca. 4.45 Ma (Morgan and McIntosh, 2005).

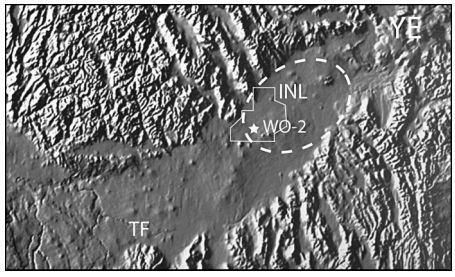

Figure 1. Digital topographic map of central and eastern Snake River Plain (SRP), southern Idaho, showing location of Idaho National Laboratory site (INL; outline), core hole WO-2 (white star), and Heise volcanic complex (dashed outline). Note abrupt termination of Basin and Range structural trends at margins of SRP, which trends NE and culminates at Yellowstone (YE) plateau. TF—Twin Falls.

The eastern Snake River Plain is underlain by a mid-crustal layer ~10 km thick and ~90 km wide that has a seismic velocity (Vp ~ 6.5 km/s) intermediate between the granulitic lower crust and more felsic upper crust (Braile et al., 1982; Peng and Humphreys, 1998). The mid-crustal layer has been interpreted to represent a sill formed by the intrusion of basaltic magma into the middle crust, but it is not possible to distinguish a single 10-km-thick sill from a sill complex consisting of many semi-contiguous sills intruded over a prolonged time. McQuarrie and Rodgers (1998) and Rodgers et al. (2002) proposed that downwarping of the eastern Snake River Plain is driven by sinking of the excess mass in this mid-crustal sill, which is found only under the eastern Snake River Plain and is absent from adjacent crust.

METHODS

We selected 59 whole-rock samples for analysis, representing all 38 major basalt flow groups documented in the core. Major elements were analyzed by fused bead electron microprobe analysis, and trace elements were

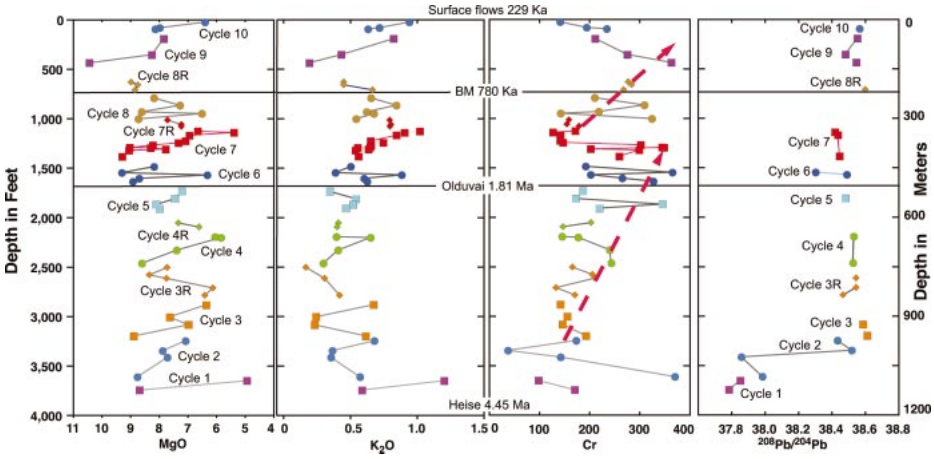

Figure 2. Plots of chemical and isotopic composition as a function of depth below surface (in feet) for MgO wt%, K_2O wt%, Cr ppm, and $^{208}Pb/^{204}Pb$ isotopic composition. Data define 10 upward enrichment cycles (decreasing MgO, Cr; increasing TiO_2 and K_2O), and four crude reversals, which are thought to represent progressive fractionation of basaltic magma in the mid-crustal magma chamber, and replenishment of this system with new magma, respectively. Note upward increase in Cr, which forms at least two megacycles (shown by red arrows) that cannot be attributed to simple fractionation.

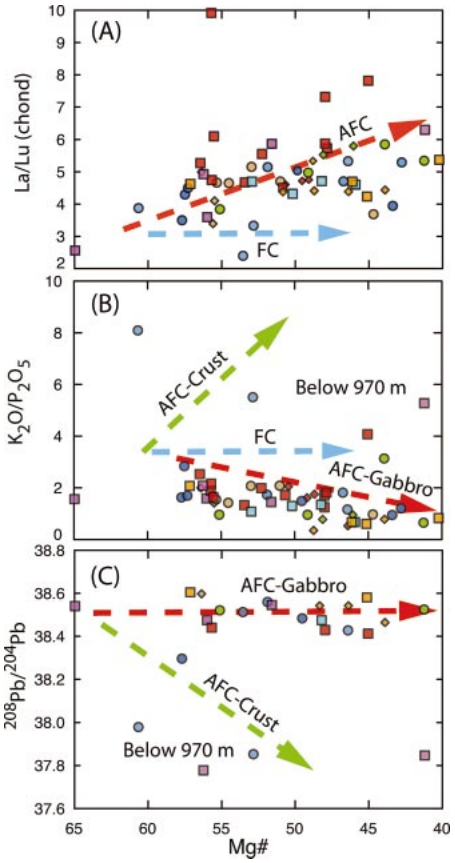

Figure 3. Ratio plots of Mg# (100*Mg/[Mg + Fe]) vs. La/Lu (chondrite normalized), K_2O/P_2O_5, and $^{208}Pb/^{204}Pb$ isotopic ratios. A: Increase in La/Lu with decreasing Mg# suggests assimilation of crustal component during fractionation (arrow). B: Decrease in K_2O/P_2O_5 shows that assimilant was rich in P_2O_5 (and other high field strength elements) relative to K_2O (and other felsic components); arrows show expected paths for fractional crystallization (FC), fractional crystallization with assimilation of felsic crust (AFC-crust), and fractional crystallization with assimilation of previously intruded basalt (AFC-gabbro); altered samples from cycle 3R are not shown. C: Relatively constant $^{208}Pb/^{204}Pb$ ratios imply that assimilant had isotopic composition similar to intruded magma, and could not represent old continental crust.

analyzed by X-ray fluorescence spectrometry and by inductively coupled plasma mass–spectroscopy; three samples are altered and have been excluded from the data set (for details see Data Repository Table DR1[1]).

RESULTS

Plots of fractionation index versus depth show that at least 10 upward fractionation series can be identified within the 1136 m of basalt core. The upward fractionation cycles are defined by decreases in MgO and Cr upsection, and by increases in FeO*, K_2O, TiO_2, P_2O_5, Zr, La, and La/Lu (e.g., MgO, K_2O, Cr; Fig. 2). The plagiophile elements CaO, Al_2O_3, and Na_2O vary more irregularly, possibly reflecting plagioclase flotation in some cumulates. Transitions between evolved compositions at the top of one cycle and primitive compositions at the base of the superjacent cycle may be abrupt or gradual; the gradual transitions are represented by reversed cycles in which the basalts become progressively more primitive upsection. There are four of these reversed cycles that occur above normal cycles 3, 4, 7, and 8 (cycles 3R, 4R, 7R, and 8R; Fig. 2). Cr concentrations define two or three megacycles above 970 m depth superimposed on the upward fractionation trends (Fig. 2).

Basalts from cycles 1 and 2 (below ~970 m depth) display wide fluctuations in major element, trace element, and isotopic compositions that are difficult to correlate with simple fractionation or recharge. For example, K_2O/P_2O_5 ratios vary from 1.2 to 8.1 below 970 m, but in the cycles above 970 m depth K_2O/P_2O_5 ratios vary from ~0.4–2.5, with a few alteration-induced fluctuations. Below 970 m depth, $^{208}Pb/^{204}Pb$ = 37.8–38.6 and $^{87}Sr/^{86}Sr$ ranges from 0.7063 to 0.7083; above 970 m depth, $^{208}Pb/^{204}Pb \geq 38.3$ and $^{87}Sr/^{86}Sr$ ranges from 0.7061 to 0.7075 ($^{208}Pb/^{204}Pb$: Fig. 2; see also Table DR1 [see footnote 1]).

The negative correlation of La/Lu with Mg# implies that assimilation was concurrent with fractional crystallization, but K_2O/P_2O_5 (and K_2O/TiO_2) ratios correlate positively with Mg# from 970 m toward the surface (Fig. 3). Thus, the assimilant must have been enriched in Ti, P, and the light rare earth elements relative to the lithophile elements that dominate normal sialic crust. Further, the relatively constant radiogenic isotope ratios above 970 m depth show that the assimilant must have had an isotopic composition similar to the parent magmas of the intruded basalts (Fig. 3).

DISCUSSION

Layered Mafic Intrusion Paradigm

The cyclic repetition of phase assemblages and compositions observed in layered mafic intrusions has long been interpreted as the response of a basaltic magma to fractional crystallization and magma recharge (e.g., Wager and Brown 1967; Jackson, 1970, 1971; Irvine, 1970; McBirney and Noyes, 1979; Pallister and Hopson, 1981). Progressive changes in phase assemblages and/or compositions within each cycle represent the instantaneous crystal extracts from an evolving magma. Changes in phase assemblages represent interception of a new phase volume, while changes in phase compositions (the so-called cryptic layering of cumulate rock assemblages) represent the progressive evolution of the magma toward lower temperatures. In contrast, the repetition of cycles involving the same or broadly similar phase assemblages upsection has been shown to represent an influx of primitive magma that mixes with any residual magma remaining in the system and draws the system back toward its original starting point. This recharge of an evolved magma with new primitive melt is the most important factor in forming the repetitive cycles that are characteristic of layered mafic intrusions (e.g., Irvine, 1970). Careful analysis of these repeated cycles has shown in several cases that assimilation of the adjacent wall rock must be operating to pull these mixed

[1]GSA Data Repository item 2006072, Table DR1, is available online at www.geosociety.org/pubs/ft2006.htm, or on request from editing@geosociety.org or Documents Secretary, GSA, P.O. Box 9140, Boulder, CO 80301, USA.

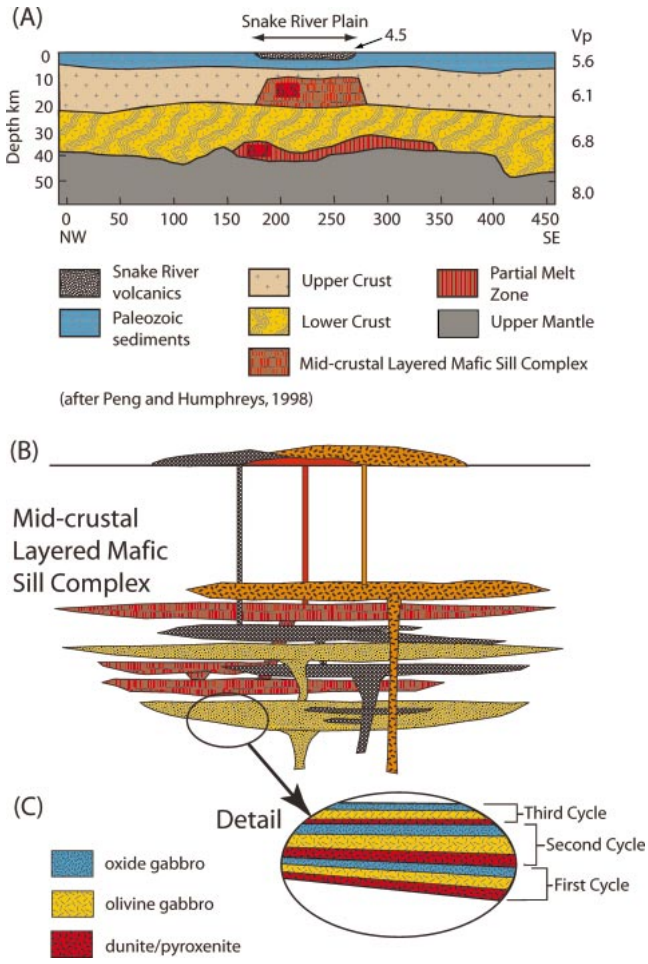

Figure 4. Model cross sections of crust with sill complex. A: Seismic velocity model of Peng and Humphreys (1998), showing location and thickness of inferred mafic sill complex. B: Detailed schematic with our interpretation of mafic sill complex as interpreted from compositional trends in lavas; separate magma batches may pond at more than one level in crust and may interact with partial melts or residual melts in partly congealed Fe-Ti basalt cumulates prior to replenishment. C: Inset showing detail of layered sill with multiple fractionation cycles forming layered intrusion; repeated cycles form in response to magma replenishment.

magmas off simple mixing trends (e.g., Jackson, 1970, 1971).

Origin of Depth-Related Variations in the Basalts

The depth-correlated variations in basalt chemistry described here imply the superposition of several different enrichment and/or fractionation mechanisms that operated with different periodicities and at different rates throughout the section. Based on our examination of these data, we can surmise that these processes included fractional crystallization, assimilation, and recharge by primitive magmas. These are the same processes inferred from phase relations observed in layered mafic intrusions (e.g., Irvine, 1970).

The upward fractionation cycles are consistent with fractional crystallization of the more primitive (high Mg#, low incompatible elements) lavas in each cycle, as confirmed by forward modeling using MELTs (Ghiorso and Sack, 1995) and Comagmat (Ariskin et al., 1993). There are distinct variations between some cycles, showing that the same parent magma cannot be used for all cycles. In particular, basalts in the upper 130 m of core require a distinct parent magma, with higher Mg#, CaO, and Al_2O_3, and lower FeO*, TiO_2, and K_2O at a given MgO content, that is unrelated to basalts lower in the core. Cr concentrations define two or three megacycles, each of which may represent a distinct magma stem (Fig. 2).

Transitions between some upward fractionation cycles are not abrupt, but occur gradationally over 30–60 m of section (cycles 3R, 4R, 7R, 8R). We infer that these gradual reversals are due to magma recharge; the gradational transitions imply that the influx of new magma batches occurred over a period of time, and did not completely overwhelm residual magma from the previous fractionation cycle. In contrast, abrupt transitions from evolved to primitive compositions imply a complete turnover in the magma supply, consistent with observations in many layered intrusions for a return to phase assemblages and compositions that are as primitive as the basal cumulates in the underlying cycle (e.g., Irvine, 1970). Alternatively, abrupt reversals may represent tapping of a new magma storage chamber, or nonuniform distribution of the erupted lava.

Assimilation of Consanguineous Basalt Intrusions: The Sill Complex as a Reactive Filter

The changes displayed by incompatible element ratios in response to decreasing Mg# require that assimilation occurred in concert with fractional crystallization, but the constant isotopic compositions above 970 m depth require that the assimilant had an isotopic composition similar to the intruded magma (Fig. 3). This assimilant could not have been older continental crust, which is characterized by high K_2O, high $^{87}Sr/^{86}Sr$ isotopic ratios, and low $^{208}Pb/^{204}Pb$ ratios. We propose that above 970 m depth, the assimilant was a partially crystallized ferrogabbro derived from a parent magma that was the same or similar to the recharge magmas. Melts derived from this ferrogabbro, or residual melts in the interstices of partially crystallized cumulates, will have isotopic compositions similar to the primitive recharge magma, but will be enriched in FeO, TiO_2, P_2O_5, and La/Lu (Fig. 3). The observed increase in K_2O/P_2O_5 upsection in the core thus represents a progressive decrease in assimilation through time, probably in response to earlier melt extraction and/or assimilation events that depleted the crust in low melting components (e.g., Geist et al., 2002).

It is unlikely that each new batch of primitive magma feeding the layered complex was identical in composition to previous batches of magma, even if they are broadly similar; each magma batch was likely to reflect small variations in source composition and percent melting, as proposed by Hughes et al. (2002). The occurrence of the reversed fractionation cycles, however, implies that these individual magma batches did not erupt directly at the surface, but were processed through a crustal storage system.

Layered Mafic Sill Complex in the Middle Crust

Where layered mafic intrusions are sufficiently well exposed, it can be shown that their form factor is sill-like, either as a funnel-shaped lopolith or as true sills that have significant horizontal extent. Less commonly described are sill complexes that represent the progressive migration of melts upward through the crust, pausing to fractionate and assimilate at crustal depths where the magma is neutrally buoyant (e.g., Marsh, 2004).

Based on the chemical stratigraphy of the NPRE and WO-2 cores, we propose that the 10-km-thick ‘‘sill’’ imaged seismically below the eastern Snake River Plain represents a complex of layered mafic sills that are partially interconnected, each feeding one or more major volcanic centers on the surface (Fig. 4). The presence of reversed cycles between some normal cyclic units implies magma recharge within a layered intrusion. The lack of reversed cycles between other normal cycles may indicate eruptions from a distinct unrelated sill, or a complete recharge of the sill that flushes out any residual melt. Alter-

natively, it could result from the fact that drill core is an imperfect record of basaltic volcanism: shield volcanoes may remain emergent for hundreds of thousands of years on one flank while being inundated by an adjacent volcano on another flank, and a drill core penetrating what was the emergent flank will record a hiatus in deposition even though volcanism was continuous.

Upward enrichment megacycles in the compatible element Cr, along with abrupt changes in incompatible elements, suggest that at least three large magma systems were present under the eastern Snake River Plain at this location; we speculate that these represent three layered sill complexes. Other layered sills are probably present along strike in the plain, to the NE and SW.

CONCLUSIONS

The preservation of chemical cycles in erupted lavas that are consistent with formation in layered mafic intrusions represents a unique confirmation of petrologic theory. The importance of layered mafic sill complexes in controlling magma evolution was highlighted by Marsh (2004), and the fact that a 10-km-thick ''sill'' has been imaged seismically below the lavas studied here confirms the validity of this model.

Because magmas will tend to pond near their depth of neutral buoyancy and thus interact with previously ponded melts and their solidified extracts, assimilation of this consanguineous material is virtually assured. The sill complex thus becomes a reactive filter that affects any magmas that attempt to traverse it on their way to the surface, forcing assimilation of previously intruded magmas (now largely crystallized to ferrogabbros) and crystallization of the equilibrium phase assemblage. This model is fundamentally the same as that proposed by Bédard (1993) for oceanic crust.

Our data show that it is possible for basaltic melts to traverse thick sections of continental crust without substantially interacting with the granitic to dioritic gneisses that dominate this crust. The data imply that once a robust conduit system has been established through the felsic crust, the ascending melts are protected from interacting with this crust by armoring of the conduit walls.

ACKNOWLEDGMENTS

This work was supported by collaborative National Science Foundation grants EAR-9526594 (Shervais), EAR-9526722 (Vetter), and EAR-9526723 (Hanan), and by U.S. Geological Survey–Edmap grants. Insightful reviews by Dennis Geist, James Beard, and William Hart helped to clarify our thinking.

REFERENCES CITED

Ariskin, A.A., Frenkel, M.Y., Barmina, G.S., and Nielsen, R.L., 1993, Comagmat: A Fortran program to model magma differentiation processes: Computers & Geosciences, v. 19, p. 1155–1170, doi: 10.1016/0098-3004(93)90020-6.

Bédard, J.H., 1993, Oceanic crust as a reactive filter; synkinematic intrusion, hybridization, and assimilation in an ophiolitic magma chamber, western Newfoundland: Geology, v. 21, p. 77–80, doi: 10.1130/0091-7613(1993)021<0077:OCAARF>2.3.CO;2.

Braile, L.W., Smith, R.B., Ansorge, J., Baker, M.R., Sparlin, M.A., Prodehl, C., Schilly, M.M., Healy, J.H., Mueller, S., and Olsen, K.H., 1982, The Yellowstone–Snake River plain seismic profiling experiment; crustal structure of the eastern Snake River plain: Journal of Geophysical Research, v. 87, no. B4, p. 2597–2609.

Champion, D.E., Lanphere, M.A., Anderson, S.R., and Kuntz, M.A., 2002, Accumulation and subsidence of the Pleistocene basaltic lava flows of the eastern Snake River Plain, Idaho, *in* Link, P.K., and Mink, L.L., eds., Geology, hydrogeology, and environmental remediation; Idaho National Engineering and Environmental Laboratory, eastern Snake River Plain, Idaho: Geological Society of America Special Paper 353, p. 175–192.

Geist, D.J., Sims, E.N., Hughes, S.S., and McCurry, M., 2002, Open-system evolution of a single episode of Snake River Plain magmatism, *in* Link, P.K., and Mink, L.L., eds., Geology, hydrogeology, and environmental remediation; Idaho National Engineering and Environmental Laboratory, eastern Snake River Plain, Idaho: Geological Society of America Special Paper 353, p. 193–204.

Ghiorso, M.S., and Sack, R.O., 1995, Chemical mass transfer in magmatic processes. IV. A revised and internally consistent thermodynamic model for the interpolation and extrapolation of liquid-solid equilibria in magmatic systems at elevated temperatures and pressures: Contributions to Mineralogy and Petrology, v. 119, p. 197–212.

Hughes, S.S., McCurry, M., and Geist, D.J., 2002, Geochemical correlations and implications for the magmatic evolution of basalt flow groups at the Idaho National Engineering and Environmental Laboratory, *in* Link, P.K., and Mink, L.L., eds., Geology, hydrogeology, and environmental remediation; Idaho National Engineering and Environmental Laboratory, eastern Snake River Plain, Idaho: Geological Society of America Special Paper 353, p. 151–173.

Irvine, T.N., 1970, Crystallization sequences in the Muskox intrusion and other layered intrusions, *in* Symposium on the Bushveld Igneous complex and other layered intrusions: Geological Society of South Africa Special Publication 1, p. 441–476.

Jackson, E.D., 1970, The cyclic unit in layered intrusions—A comparison of repetitive stratigraphy in the ultramafic parts of the Stillwater, Muskox, Great Dyke, and Bushveld complexes, *in* Symposium on the Bushveld Igneous complex and other layered intrusions: Geological Society of South Africa Special Publication 1, p. 391–424.

Jackson, E.D., 1971, The origin of ultramafic rocks by cumulus processes: Fortschritte Der Mineralogie, v. 48, p. 128–174.

Leeman, W.P., 1982, Development of the Snake River Plain–Yellowstone Plateau province, Idaho and Wyoming: An overview and petrologic model, *in* Bonnichsen, B., and Breckenridge, R.M., eds., Cenozoic geology of Idaho: Idaho Bureau of Mines and Geology Bulletin 26, p. 155–177.

Marsh, B., 2004, A magmatic mush column Rosetta Stone: The McMurdo Dry Valleys of Antarctica: Eos (Transactions, American Geophysical Union), v. 85, p. 497–508.

McBirney, A.R., and Noyes, R.M., 1979, Crystallization and layering of the Skaergaard Intrusion: Journal of Petrology, v. 20, p. 487–554.

McQuarrie, N., and Rodgers, D.W., 1998, Subsidence of a volcanic basin by flexure and lower crustal flow, the eastern Snake River plain, Idaho: Tectonics, v. 17, p. 203–220, doi: 10.1029/97TC03762.

Morgan, L.A., and McIntosh, W.C., 2005, Timing and development of the Heise volcanic field, Snake River plain, Idaho, western USA: Geological Society of America Bulletin, v. 117, p. 288–306, doi: 10.1130/B25519.1.

Morse, L.H., and McCurry, M., 2002, Genesis of alteration of Quaternary basalts within a portion of the eastern Snake River Plain Aquifer, *in* Link, P.K., and Mink, L.L., eds., Geology, hydrogeology, and environmental remediation; Idaho National Engineering and Environmental Laboratory, eastern Snake River Plain, Idaho: Geological Society of America Special Paper 353, p. 213–224.

Pallister, J.S., and Hopson, C.A., 1981, Samail ophiolite plutonic suite; field relations, phase variation, cryptic variation and layering, and a model of a spreading ridge magma chamber, *in* Coleman, R.G., and Hopson, C.A., eds., Oman ophiolite: Journal of Geophysical Research, p. 2593–2644.

Peng, X., and Humphreys, E.D., 1998, Crustal velocity structure across the eastern Snake River plain and the Yellowstone Swell: Journal of Geophysical Research, B, Solid Earth and Planets, v. 103, no. 4, p. 7171–7186, doi: 10.1029/97JB03615.

Rodgers, D.W., Ore, H.T., Bobo, R.T., McQuarrie, N., and Zentner, N., 2002, Extension and subsidence of the eastern Snake River plain, Idaho, *in* Bonnichsen, B., et al., eds., Tectonic and magmatic evolution of the Snake River Plain volcanic province: Idaho Geological Survey Bulletin 30, p. 121–156.

Shervais, J.W., Hanan, B.B, and Vetter, S.K., 2003, Chemical stratigraphy of basalts from the 5000′ borehole NPR-E/WO-2, eastern Snake River Plain, Idaho: Evidence for mixed asthenosphere-lithosphere sources. Eos (Transactions, American Geophysical Union), v. 84, fall meeting supplement, abs. V32H–03.

Shervais, J.W., Kauffman, J.D., Gillerman, V.S., Othberg, K.L., Vetter, S.K., Hobson, V.R., Meghan Zarnetske, M., Cooke, M.F., Matthews, S.H., and Hanan, B.B., 2005, Basaltic volcanism of the central and western Snake River Plain: A guide to field relations between Twin Falls and Mountain Home, Idaho, *in* Pederson, J., and Dehler, C.M., eds., Guide to field trips in the western United States: Geological Society of America Field Guide, v. 6, p. 27–52.

Wager, L.R., and Brown, G.M., 1967, Layered igneous rocks: San Francisco, California, W.H. Freeman and Company, 588 p.

Manuscript received 25 September 2005
Revised manuscript received 13 December 2005
Manuscript accepted 19 December 2005

Printed in USA

Seamount subduction erosion in the Nankai Trough and its potential impact on the seismogenic zone

Nathan L.B. Bangs
Sean P.S. Gulick
Thomas H. Shipley
Institute for Geophysics, University of Texas at Austin, 4412 Spicewood Springs Road, Austin, Texas 78759, USA

ABSTRACT

Seamount subduction along subduction-zone plate boundary thrusts has long been implicated as a mechanism for abrasion and tectonic erosion of the base of the overriding plate. However, tectonic erosion processes have not been examined in detail with high-quality three-dimensional (3-D) seismic reflection imaging. In 1999 we acquired 3-D seismic reflection data from the Nankai Trough subduction zone to image the plate boundary fault and the overlying accretionary wedge structure. Fortuitously, these data reveal a small (to 1 km high) basement ridge that has subducted to 7 km subseafloor. Updip from the basement ridge, a 1-km-thick sequence of sediment from the base of the accretionary wedge appears to be missing. We interpret these data as evidence for tectonic erosion of the base of the accretionary wedge following the basement ridge subduction. Tectonic erosion has removed more than 25 km^3 from the updip edge of the seismogenic zone and carried it down into the seismogenic zone. The tectonically eroded sediments are presumed to enhance fault-zone fluid content, potentially reducing fault-zone effective stress, and may temporarily inhibit earthquake rupture potential. After the passage of the ridge the boundary fault returns to its former position in a period of enhanced underplating.

Keywords: seamount subduction, tectonic erosion, seismogenic zone, Nankai Trough, subduction zone.

INTRODUCTION

Seamounts and basement ridges on subducting ocean crust have large direct impacts on subduction-zone structures and processes as they collide with overriding plates in subduction zones. The most apparent effects are the distinctive furrows in the lower slope of the overriding plate; the furrows form as the seamount is thrust into the subduction zone and thus track the path of a subducting seamount (e.g., von Huene et al., 2000). However, many effects along the plate boundary are less visible because seamounts cause significant abrasion that leads to subduction erosion (specifically basal erosion) of the overriding plate (Ranero and von Huene, 2000). The buoyancy of seamounts also alters subduction-zone thrust stresses that can generate asperities for great subduction-zone earthquakes (Cloos, 1992; Cloos and Shreve, 1996; Scholz and Small, 1997). Seamount subduction is common in the world's subduction zones; several well-studied examples include Middle America (McIntosh et al., 2005; Ranero and von Huene, 2000), the Japan Trench (Lallemand et al., 1989, 1994), the Chile margin (Yañez et al., 2001), and the Nankai Trough (Park et al., 1999; Kodaira et al., 2000, 2002).

While seamount subduction has a potentially significant impact on structures and processes along the subduction thrust, there is still little known about how seamounts abrade the overriding plate and generate earthquake asperities as they are subducted. Previous studies of the mechanisms by which seamounts erode the base of the overriding plate in subduction zones have been limited to interpretation of structures observed in sandbox models (e.g., Dominguez et al., 1998, 2000), a few two-dimensional (2-D) seismic profiles that have imaged seamounts in the subduction zone (Park et al., 1999; McIntosh et al., 2005; Ranero and von Huene, 2000; von Huene et al., 2000), and three-dimensional (3-D) observations of imbricate thrust geometry formed in the wake of a seamount (Gulick et al., 2004). Little is known about the mechanisms and processes of seamount tectonic erosion in subduction zones because the structural details needed to interpret them are too deep and complex to image well with 2-D seismic imaging.

In 1999 we acquired 3-D seismic reflection data across the Nankai Trough south of the Muroto Peninsula (Fig. 1[1]) (Bangs et al., 2004). For the first time, 3-D data have fortuitously captured images of a subducting seamount, part of the Kinan seamount chain, after it passed beneath the Nankai Trough accretionary wedge and entered into the seismogenic zone (Fig. 2; see footnote 1). Here we present 3-D images of the structures formed in the wake of a subducting seamount near the updip edge of the seismogenic zone to interpret the impact of seamount subduction on subduction-zone structure and infer its impact on the development of the seismogenic zone.

DEEP STRUCTURES IN THE MUROTO TRANSECT

We acquired an 8×80 km^2 volume of 3-D seismic reflection data to investigate the aseismic to seismic transition of the décollement from the trench into the seismogenic zone along the Nankai Trough, offshore southwestern Japan. Data acquisition and a prestack time migrated volume were described and presented in Bangs et al. (2004). Although the prestack time migrations were sufficient to image structures within the imbricate thrust zone (defined in Fig. 2; see footnote 1) reasonably well, clearer images of deeper structures were needed to fully interpret the structure of the accretionary wedge and subducting oceanic crust. We improved images within complex structures by contracting Paradigm Geophysical to conduct a 3-D prestack depth migration of the data volume (Fig. 2), specifically targeting the structures beneath the steep seafloor slopes of the large-thrust-slice zone (Fig. 2). Prestack depth migration in 3-D significantly improved cross-line

[1]Figures 1–3 are on a separate insert accompanying this issue.

(strike direction) seismic sections to allow 3-D structural interpretation of the stratigraphic horizons within thrust sequences (Fig. 3; see footnote 1). The results presented here are based on these 3-D prestack depth migrated data.

SUBDUCTING OCEAN CRUST

We can trace the subducting ocean crust as a high-amplitude seismic reflection beneath the accretionary wedge from the trench to the landward edge of the survey, 70 km from the toe of the accretionary wedge and 1–7 km below seafloor (Fig. 2; see footnote 1). The top of ocean crust typically has 100–200 m of relief throughout the volume, with a notable exception. A significant basement ridge is ~65 km landward from the wedge toe beneath a local bathymetric high on the seafloor. This structure is ~5 km wide in the dip direction with as much as 1 km relief in our 3-D volume. The 1 km relief of the basement ridge is twice the thickness of the underthrust sediment section observed beneath most of the accretionary wedge farther seaward. In the strike direction, the basement ridge extends the full 8 km width of the 3-D data volume (Figs. 3C, 3D; see footnote 1), but it tapers from ~1 km relief on the SW edge of the survey down to 100–200 m on the NE boundary. This basement ridge is likely part of the Kinan seamount chain associated with oceanic crust formation (Kobayashi et al., 1995) proximal to a much larger subducting seamount that produced Tosa-bae to the NE (Fig. 1; see footnote 1) (Kodaira, et al., 2000; Gulick et al., 2004) and a slightly larger subducted seamount observed to the SW (Fig. 1) (Park et al., 1999).

ACCRETIONARY WEDGE THRUSTS

Three main thrust units comprise the large-thrust-slice zone of the accretionary wedge (Figs. 2 and 3; see footnote 1) previously defined by Moore et al. (2001a). These thrusts are recognizable as distinctly separate units of tilted and deformed stratigraphic sequences. We interpret these thrusts as primary thrusts because they extend from the main plate boundary thrust (décollement) at the base of the accretionary wedge through the entire wedge to the seafloor. These thrusts are also traceable in the strike (cross line) direction as a continuous surface across the entire 8 km width of the 3-D volume in the prestack depth migrated data.

Figure 3 illustrates a significant structural change in the geometry along strike of these primary thrusts. Along the SW inline (dip direction) transect (inline 207 in Fig. 3A), the red and orange thrusts are steeply dipping in the upper two-thirds of the accretionary wedge and mostly flat lying within the lower third, especially in comparison to the NE transect (inline 292 in Fig. 3B). Along the SW transect, the seawardmost fault (red in Fig. 3A) soles out ~500 m above the décollement and ~1000 m above the top of subducting ocean crust. At its base, the red thrust is parallel to the décollement for more than 5 km. In the strike direction, each thrust dips SW (toward inline 199 in Fig. 3C) in the uppermost two-thirds of the wedge, and dips NE (toward inline 348) near the base of the accretionary wedge (Figs. 3B, 3D). Reflections from the stratigraphic horizons also follow the same dip changes from the top to bottom of the accretionary wedge, especially for the section between the orange and red faults (Figs. 3C, 3D). These faults have a twisted or ''corkscrew'' geometry in 3-D (i.e., SW dipping in the shallow section and NE dipping at the base) that is inconsistent with shortening parallel to plate convergence (the dip direction).

MISSING SECTION

Cross-line profiles through the 3-D prestack depth migrated data show strong evidence for a missing stratigraphic section between the orange and red thrust faults (Figs. 3C, 3D; see footnote 1). Stratigraphic horizons between the orange and red thrusts can be traced to the SW where they are truncated by the red thrust. The red thrust appears to step up into the stratigraphic section between these thrusts. The separation between the deepest and shallowest horizons intersected by the red thrust is ~1000 m (Fig. 3D). We interpret this as ~1000 m of missing section of this thrust package and note that thickness and shape of this missing sequence are very similar to those of the subducted basement ridge described here.

BASAL SECTION

The décollement is recognizable as a high-amplitude reflection that parallels the top of the subducting ocean crust (see Bangs et al., 2004). Along the NE edge of the 3-D volume (inlines 348 and 292; Fig. 3), thrusts sole out into the décollement where it is ~500 m from the top of oceanic crust. However, along the SW transect (inlines 199 and 207; Fig. 3) these faults sole out at much shallower depths, ~1000 m above the top of ocean crust. A wedge-shaped section (yellow shading in Fig. 3), which is ~500 m at its thickest along the SW transect, is between the red thrust and the décollement. There are numerous horizontal seismic reflections within this section that are not parallel to the overlying horizons comprising the thrust packages. This interval was interpreted (Bangs et al., 2004) as an underplated sediment section. The 3-D prestack depth images support that interpretation and reveal the 3-D geometry of this interval.

INTERPRETATION

The 3-D volume reveals the effects of ridge subduction in greater detail than has been observed previously. As the ridge approached the accretionary wedge it steepened the overlying thrusts. Along the SW profile of the 3-D volume (i.e., inline 207 in Fig. 3A; see footnote 1) where the basement ridge is highest (~1 km), thrusts are noticeably steeper in the shallow section than to the NE (i.e., inline 292 in Fig. 3B). The steeper thrusts are presumably due to greater thickening where the basement relief of the seamount met the accretionary wedge. Observations and models of seamount subduction show wedge thrusting and thickening in front of the path of the subducting seamount as a primary effect of seamount subduction (Park et al., 1999; Dominguez et al., 2000).

From the inferred missing stratigraphic sequences within the accretionary wedge and the geometry of the accretionary wedge thrusts, we infer that a tapered wedge of rock ~100 m thick on the NE edge of the 3-D volume and 1000 m thick on the SE edge has been tectonically eroded from the base of the accretionary wedge. Removal of a tapered wedge of material from the base of the accretionary wedge would cause the apparent subsidence of these structures and produce the peculiar cross-line dip observed in the large-thrust-slice zone. Usually accretionary wedge thrusts are nearly horizontal in the strike direction, as Gulick et al. (2004) found in recently formed thrusts within the imbricate thrust zone farther seaward. We presume that the cross-line dip is not an inherent structure, but is caused by tectonic erosion from the base of the accretionary wedge after these thrusts formed.

Coincidentally, the subducting basement ridge corresponds well with both the height of inferred missing accretionary wedge section and its shape. The inferred missing sequence is as thick as 1000 m and tapers to the NE, coincident with the shape of the basement ridge to within the limits of uncertainty in the interpretation (100–200 m). We speculate that as the basement ridge passed beneath the accretionary wedge, it removed a section from the base of the accretionary wedge.

A lens-shaped body, the basal section described herein (shaded yellow in Fig. 3), is between the base of the tectonically eroded section and the décollement. The stratigraphic horizons within this layer are consistently discordant with the overlying strata, which led Bangs et al. (2004) to interpret this interval as an underplated layer from the

prestack time migrated data volume. What was not apparent in the earlier interpretation is that the lens-shape geometry of this layer coincides with the shape of the subducted basement ridge. The underplated layer appears to have been subducted beneath the accretionary wedge in the wake of the subducting seamount, as predicted by the models of Dominguez et al. (2000). The volume of material that we interpret to be tectonically eroded from within the 3-D volume is at least 25 km^3, approximately half of which was replaced by underplating.

DISCUSSION

A seamount or basement ridge with as much as 1 km relief and with strike parallel to the margin has subducted beneath the accretionary wedge to a position deep within the seismogenic zone, ~65 km from the present deformation front and ~7 km below the seafloor. The ridge is now well within the seismogenic zone defined by Moore and Saffer (2001). Ocean Drilling Program Leg 190 drilling at Site 1175 derived an age of <2 m.y. (Moore et al., 2001b) for the accretionary wedge at the landward edge of the large-thrust-slice zone. The seamount would have been located ~10 km seaward of the present deformation front at 2 Ma, when accretion of the large-thrust-slice zone began. This relationship implies that while most of the imbricate thrust zone probably formed behind the path of the subducting ridge and was unaffected by it, the subducting ridge collided directly with the large-thrust-slice zone soon after, or as, it was accreted to the overriding plate. The results of that collision are now observed in our 3-D data volume.

The primary effect of ridge collision is tectonic erosion from the base of the accretionary wedge. The missing section and the corkscrew geometry of the thrust faults are strong evidence that the décollement stepped up into the accretionary wedge ahead of the subducting basement ridge to cause a significant section of the accretionary wedge to become attached to the subducting plate ahead of the subducting basement ridge. Further subduction caused the tectonic removal of as much as 1 km of the upper plate (Fig. 4). The downdip extent of this upward shift of the décollement was probably >10 km, which we can infer from the observation that erosion extends beneath the entire large-thrust-slice zone. The upward step of the décollement into the overriding plate is analogous to the formation of megalenses that are interpreted as a mechanism for tectonic erosion of the Costa Rican margin (Ranero and von Huene, 2000); however, in this instance the upward décollement step is directly induced by the basement topography, analogous to the physical abrasion mechanism of tectonic erosion proposed by Hilde (1983).

While basal erosion observed here may be equivalent to the process that forms megalenses described by Ranero and von Huene (2000), they observed significant collapse of the margin in the wake of the tectonic erosion, which is not observed here. We observe both an underplated and an underthrust section that has replaced the tectonically eroded material in the wake of the subducting seamount and prevented much of the collapse of the overriding accretionary wedge. The bite taken out of the accretionary wedge here conforms directly to the geometry of the basement ridge, closely following the model by Hilde (1983), and does not appear to follow as directly the generic model of tectonic erosion by upward migration of the décollement following pore fluid injection into the overriding plate proposed by von Huene et al. (2004). The lack of furrows in the seafloor morphology in the wake of the seamount is because the repositioning of the fault and the underplating must be occurring more efficiently than in some other margins. This may be related to fluid content and loading of the underthrust section beneath the steep seafloor of the large-thrust-slice zone, but we can only speculate on the conditions that existed when the seamount was updip 20–30 km (500–750 k.y. ago).

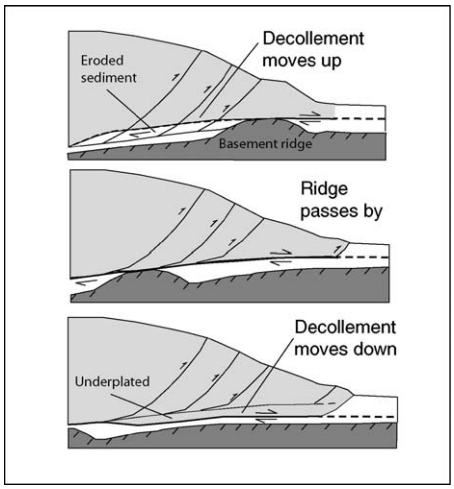

Figure 4. Schematic models of basement ridge subduction sequence and resulting tectonic erosion inferred from three-dimensional (3-D) seismic images and sandbox models of Dominguez et al. (2000). Top panel: décollement (thin solid line) at base of accretionary wedge (light gray) steps up into accretionary wedge (dashed line) and intersects pre-existing accretionary wedge thrusts. Middle panel: décollement remains high as ridge passes by and in wake of subducting seamount. Bottom panel: décollement (thin solid line) steps down into underthrust section (thick solid line) to underplate thick section of sediment to base of accretionary wedge.

What remains unclear is where has the tectonically eroded section gone and how is it affecting the seismogenesis? There is strong evidence for tectonic erosion; however, there are no clues in the seismic images that show where the tectonically eroded material is now. Was the eroded material underplated to the base of the accretionary wedge downdip from where it was removed, or is it still attached to the subducting plate in front of the basement ridge? If material composition is a major control on seismogenesis, as suggested by Moore and Saffer (2001), then redistributing a large volume of relatively high-porosity sediment from the updip edge of the seismogenic zone down into the seismogenic zone could introduce pore fluids into the seismogenic zone and reduce effective stress and thus lower earthquake potential, at least temporarily. Seismic velocities from prestack depth processing are currently ~3.2 km/s in the vicinity of the observed tectonic erosion, from which a porosity of 20%–30% (Nafe and Drake, 1960) is inferred. Therefore, a significant volume of pore fluid from the eroded sediment is potentially available for interacting with the subduction thrust.

Seamount subduction, the resultant subduction erosion, and the potential for introducing fluids into the seismogenic zone may interfere with rupture propagation. Observations of the 1946 Nankaido Mw 8.4 event indicate that the slip initiated in two places, and rupture propagated around the subducting seamount beneath Tosa-bae. Slip inferred from tsunami inversion (Baba and Cummins, 2005) indicates that small slips of <1 m characterize the seismogenic zone updip from the Kinan seamounts, which is notably less than in adjacent portions of the rupture segment. While this could be attributed to the increased coupling of the seamount beneath Tosa-bae (Kodaira et al., 2000, 2002; Scholz and Small, 1997), Cummins et al. (2002) also proposed that damage to the upper plate prevents elastic strain accumulation necessary for

seismic rupture. Tectonic erosion and sediment subduction from seamount collision with the accretionary wedge may lead to fluids being subducted into the seismogenic zone. The delivery of fluids may inhibit accumulation of elastic strain and diminish seismic rupture updip from the subducting seamounts. Tectonic erosion and entrainment of fluid-rich materials may also have a large impact on the development of seamounts as earthquake asperities.

ACKNOWLEDGMENTS

We thank Matthew Brzostowski, Xuening Ma, Brad Beck, Jim Wilhite, and Zhiyong Zhao at Paradigm Geophysical for their efforts with prestack depth migration of these data. We are grateful to César Ranero, Demian Saffer, and an anonymous reviewer for their critical comments. This work was supported by National Science Foundation grant OCE-9730637. University of Texas Institute for Geophysics contribution 1808.

REFERENCES CITED

Baba, T., and Cummins, P.R., 2005, Contiguous rupture areas of two Nankai Trough earthquakes revealed by high-resolution tsunami waveform inversion: Geophysical Research Letters, v. 32, p. L08305, doi: 10.1029/2004GL022320.

Bangs, N.L., Shipley, T., Gulick, S., Moore, G., Kuromoto, S., and Nakamura, Y., 2004, Evolution of the Nankai Trough décollement from the trench into the seismogenic zone: Inferences from three-dimensional seismic reflection imaging: Geology, v. 32, p. 273–276.

Cloos, M., 1992, Thrust-type subduction-zone earthquakes and seamount asperities: A physical model for seismic rupture: Geology, v. 20, p. 601–604.

Cloos, M., and Shreve, R.L., 1996, Shear-zone thickness and the seismicity of Chilean- and Marianas-type subduction zones: Geology, v. 24, p. 107–110.

Cummins, P.R., Baba, T., Kodaira, S., and Kaneda, Y., 2002, The 1946 Nankai earthquake and segmentation of the Nankai Trough: Physics of the Earth and Planetary Interiors, v. 132, p. 75–87.

Dominguez, S., Lallemand, S.E., Malavieille, J., and von Huene, R., 1998, Upper plate deformation associated with seamount subduction: Tectonophysics, v. 293, p. 207–224.

Dominguez, S., Malavieille, J., and Lallemand, S.E., 2000, Deformation of accretionary wedges in response to seamount subduction: Insights from sandbox experiments: Tectonics, v. 19, p. 182–196.

Gulick, S.P.S., Bangs, N.L., Shipley, T.H., Nakamura, Y., Moore, G.F., and Kuramoto, S., 2004, 3-D architecture of the Nankai accretionary prism's imbricate thrust zone off Cape Muroto, Japan: En echelon thrust accommodation of along strike stress regime changes: Journal of Geophysical Research, v. 109, p. B02105, doi: 10.1029/2003JB002654.

Hilde, T.W.C., 1983, Sediment subduction versus accretion around the Pacific: Tectonophysics, v. 99, p. 381–397.

Kobayashi, K., Kasuga, S., and Okino, K., 1995, Shikoku basin and its margins, *in* Taylor, B., ed., Backarc basins: Tectonics and magmatism: New York, Plenum Press, p. 381–405.

Kodaira, S., Takahashi, N., Nakanishi, A., Miura, S., and Kaneda, Y., 2000, Subducted seamount imaged in the rupture zone of the 1946 Nankaido earthquake: Science, v. 289, p. 104–106.

Kodaira, S., Kurashimo, E., Park, J.-O., Takahashi, N., Nakanishi, A., Miura, S., Iwasaki, T., Hirata, N., Ito, K., and Kaneda, Y., 2002, Structural factors controlling the rupture process of megathrust earthquake at the Nankai trough seismogenic zone: Geophysical Journal International, v. 149, p. 815–835.

Lallemand, S., Culotta, R., and von Huene, R., 1989, Subduction of the Daiichi Kashima Seamount in the Japan Trench: Tectonophysics, v. 160, p. 231.

Lallemand, S.E., Schnürle, P., and Malavielle, J., 1994, Coulomb theory applied to accretionary and nonaccretionary wedges: Possible causes for tectonic erosion and/or frontal accretion: Journal of Geophysical Research, v. 99, p. 12,033–12,055.

McIntosh, K.D., Silver, E., Ahmed, I., Berhorst, A., Ranero, C.R., Kelly, R.K., and Flueh, E.R., 2005, The Nicaragua convergent margin: Seismic reflection imaging of the source of a tsunami earthquake, *in* Dixon, T., and Moore, J.C., eds., The Seismogenic Zone of Subduction Thrust Faults: New York, Columbia University Press (in press).

Moore, G.F., Taira, A., Bangs, N.L., Kuramoto, S., Shipley, T.H., Alex, C.M., Gulick, S.S., Hills, D.J., Ike, T., Ito, S., Leslie, S.C., McCutcheon, A.J., Mochizuki, K., Morita, S., Nakamura, Y., Park, J.O., Taylor, B.L., Toyama, G., Yagi, H., and Zhao, Z., 2001a, Data report: Structural setting of the Leg 190 Muroto transect, *in* Moore, G.F., et al., eds., Proceedings of the Ocean Drilling Program, Initial reports, Volume 190: College Station, Texas, Ocean Drilling Program, p. 1–14.

Moore, G.F., and 22 others, 2001b, Proceedings of the Ocean Drilling Program, Initial reports, Volume 190: College Station, Texas, Ocean Drilling Program.

Moore, J.C., and Saffer, D., 2001, Updip limit of the seismogenic zone beneath the accretionary prism of southwest Japan: An effect of diagenetic to low-grade metamorphic processes and increasing effective stress: Geology, v. 29, p. 183–196.

Nafe, J.E., and Drake, C.L., 1960, Physical properties of marine sediments, *in* Hill, M.N., ed., The sea, Volume 3: New York, Interscience, p. 794–815.

Park, J.-O., Tsuru, T., Kaneda, Y., and Kono, Y., 1999, A subduction seamount beneath the Nankai accretionary prism off Shikoku, southwestern Japan: Geophysical Research Letters, v. 26, p. 931–934.

Ranero, C.R., and von Huene, R., 2000, Subduction erosion along the Middle America convergent margin: Nature, v. 404, p. 748–752.

Scholz, C.H., and Small, C., 1997, The effect of seamount subduction on seismic coupling: Geology, v. 25, p. 487–490.

von Huene, R., Ranero, C.R., Weinrebe, W., and Hinz, K., 2000, Quaternary convergent margin tectonics of Costa Rica, segmentation of the Cocos Plate, and central American volcanism: Tectonics, v. 19, p. 314–334, doi: 10.1029/1999TC001143.

von Huene, R., Ranero, C.R., and Vannucchi, P., 2004, Generic model of subduction erosion: Geology, v. 32, p. 913–916.

Yañez, G.A., Ranero, C.R., von Huene, R., and Díaz, J., 2001, Magnetic anomaly interpretation across the southern central Andes (32°–34°S): The role of the Juan Fernández Ridge in the late Tertiary evolution of the margin: Journal of Geophysical Research, v. 106, p. 6325–6345.

Manuscript received 22 November 2005
Revised manuscript received 8 March 2006
Manuscript accepted 12 March 2006

Printed in USA

Erratum

Ultrafine-grained quartz mylonites from high-grade shear zones: Evidence for strong dry middle to lower crust

John D. Fitz Gerald, Neil S. Mancktelow, Giorgio Pennacchioni and Karsten Kunze. *Geology*: Vol. 34, No. 5, pp. 369–372 (May 2006).

In the footnote for Data Repository item 2006073, the link to the Data Repository item should have read www.geosociety.org/pubs/ft2006.htm.

In the paper, the acronym EBSD was incorrectly identified; it should have been ''electron backscattered diffraction.''

Geology

Layered mafic sill complex beneath the eastern Snake River Plain: Evidence from cyclic geochemical variations in basalt

John W. Shervais, Scott K. Vetter and Barry B. Hanan

Geology 2006;34;365-368
doi: 10.1130/G22226.1